JOURNAL OF MATERIALS SCIENCE **40** (2005) 1153– 1158

Effects of gallia additions on sintering behavior of $Ce_{0.8}Gd_{0.2}O_{1.9}$ ceramics prepared by commercial powders

JOO-SIN LEE*, KWANG-HOON CHOI
Department of Advanced Materials Engineering, Kyungsung University, Busan 608-736, Korea
E-mail: leejs@ks.ac.kr

BONG-KI RYU
School of Materials Science and Engineering, Pusan National University, Busan 609-735, Korea

BYOUNG-CHUL SHIN, IL-SOO KIM
Department of Information Materials Engineering, Dongeui University, Busan 614-714, Korea

The densification behavior and grain growth of $Ce_{0.8}Gd_{0.2}O_{1.9}$ ceramics were investigated with the gallia concentration ranging from 0 to 10 mol%. Both the sintered density and grain size were found to increase rapidly up to 0.5 mol% Ga_2O_3, and then to decrease with further additions. Under the same sintering conditions, the samples with 3 mol% Ga_2O_3 and less exhibited a higher sintered density, as compared to the one without Ga_2O_3 addition. However, a pinning effect on grain growth was found at $\geq$2 mol% Ga_2O_3. In the dopant content range of 0 to 10 mol%, 0.5 mol% Ga_2O_3 was the optimum doping level in promoting densification and grain growth of commercially available powders of $Ce_{0.8}Gd_{0.2}O_{1.9}$.

1. Introduction

Oxygen ionic conductors have a wide variety of applications in the field of electrochemistry. They can be used as solid electrolyte membranes in oxygen sensors, fuel cells, and oxygen pumps. Among the oxygen ionic conductors, Y_2O_3-stabilized ZrO_2 (YSZ) has been the most extensively investigated and practically used. However, especially for solid oxide fuel cell (SOFC) applications, a considerable research effort was devoted to developing alternative solid electrolytes for YSZ, which should possess higher electrical conductivity than YSZ and be operable at lower temperatures around 800°C.

Ceria electrolyte has received much attention as an alternative to YSZ [1]. However, ceria-based ceramics are difficult to be densified below 1600°C [2]. This makes them difficult for manufacturing ceria-based electrolytes which can be used for SOFC system because ceria-based electrolytes and other components such as cathode and anode need to be cofired.

In order to lower the sintering temperature, other methods utilizing fine starting powders and additives as sintering aids should be exploited. The preparation of ultra fine ceria-based ceramic powders has been studied by many investigators [2–9]. In contrast, only a limited number of reports are available as to the densification of ceria-based ceramics with the addition of sintering additives [10–14].

Yoshida *et al.* [10] reported that sintering of samaria-doped ceria was significantly promoted by the addition of a small amount of gallia. They reported that the samples sintered at 1450°C with the addition of 1% gallium had almost the same average grain size and electrical conductivity as the samples sintered at 1600°C without Ga_2O_3 addition.

It has been also reported that transition metal oxide additives enhance densification. The effects of cobalt oxide additions on the sintering characteristics and electrical properties of $Ce_{0.8}Gd_{0.2}O_{2-x}$ ceramics were investigated by Kleinlogel and Gauckler [11, 12]. They reported that the addition of a small amount of Co_3O_4 strongly enhanced the densification kinetics without altering the electrochemical performance of $Ce_{0.8}Gd_{0.2}O_{2-x}$ ceramics. The densification was explained by a liquid-phase sintering mechanism.

Zhang *et al.* [13, 14] investigated the effects of transition metal oxide additives on the sintering characteristics of undoped CeO_2. They reported that the addition of a small amount of Fe_2O_3 or CoO strongly enhanced the densification rate and promoted the

*Author to whom all correspondence should be addressed.

grain boundary mobility. As a result, these additives could lower the sintering temperature of CeO_2.

It should be noted that studies on the sintering additives used for ceria-based ceramics have been limited to Ga_2O_3, Co_3O_4, Fe_2O_3 and CoO additives. The starting powders used have been either commercially available powders or doped powders prepared by the conventional mixed-oxide method.

We had studied the effects of Ga_2O_3 additions on the sintering behavior of $Ce_{0.8}Gd_{0.2}O_{1.9}$ ceramics prepared by the coprecipitated powders [15]. The results are described as follows. Both sintered density and grain size increased with increasing Ga_2O_3 content up to 5 mol%. However, they decreased with further addition of Ga_2O_3 above 6 mol%. At higher Ga_2O_3 content, grain size decreased by a pinning effect of Ga_2O_3 precipitation. The solubility limit of Ga_2O_3 in $Ce_{0.8}Gd_{0.2}O_{1.9}$ ceramics estimated using the results obtained from SEM and XRD analyses was about 5 mol%. In our previous work [15], we suggested that the addition of Ga_2O_3 up to its solid solubility limit gave an affirmative effect on the sintering behavior of Gd_2O_3-doped CeO_2.

The previous work, however, was performed by the use of coprecipitated powders. It is noted that the sintering and densification behavior of ceria-based ceramics depend strongly on the characteristics of the raw powders. In the present work, high purity commercial CeO_2, Gd_2O_3 and Ga_2O_3 has been used as starting materials. The present work is aimed at studying the effects of Ga_2O_3 additions on the sintering behavior of $Ce_{0.8}Gd_{0.2}O_{1.9}$ ceramics prepared by the conventional mixed-oxide method.

2. Experimental procedure

Fig. 1 shows a schematic flow diagram of experimental procedure. Mixtures having a composition corresponding to $(Ce_{0.8}Gd_{0.2}O_{1.9})_{1-x}(Ga_2O_3)_x$ $(x = 0-0.1)$ were prepared by the conventional mixed-oxide method.

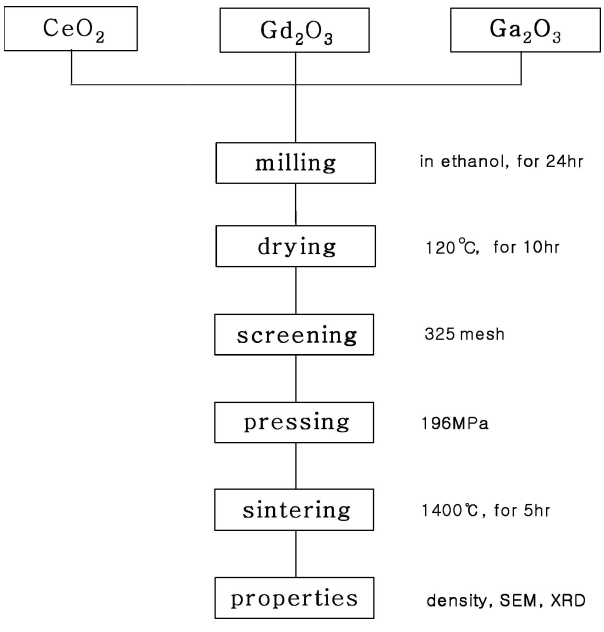

Figure 1 Flow chart of experimental procedure.

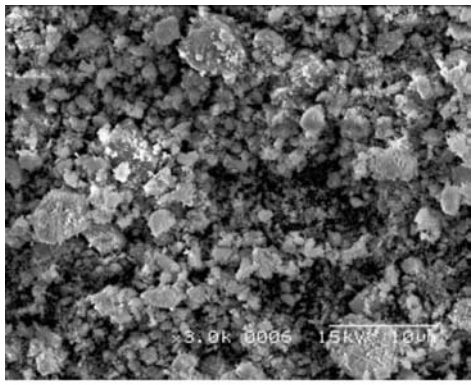

(a) CeO_2

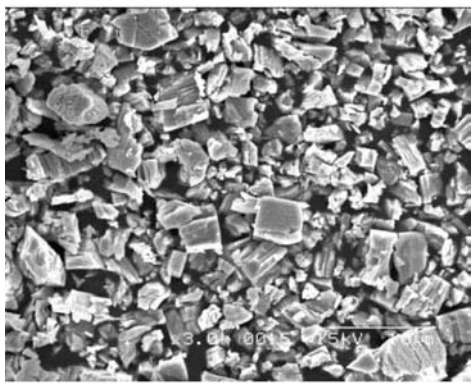

(b) Gd_2O_3

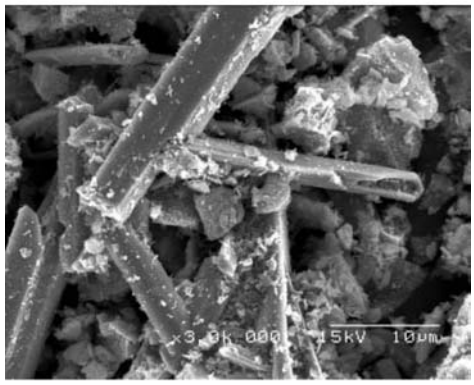

(c) Ga_2O_3

Figure 2 SEM micrographs of commercial powders.

High purity commercial CeO_2 (Aldrich Chemical Co., 99.9%), Gd_2O_3 (Aldrich Chemical Co., 99.9%), and Ga_2O_3 (Aldrich Chemical Co., 99.99%) were used as starting materials.

The CeO_2 powders consisted of particles having a size of approximately 1 μm as shown in Fig. 2a. Fig. 2 shows the SEM micrographs of commercial powders. The Gd_2O_3 powders consisted of particles having a size of approximately 3 μm. The Gd_2O_3 particles, however, contained more cracks. The Ga_2O_3 powders used as additives had the morphology of coarse elongated particles with a high aspect ratio.

The mixtures were ball-milled in ethanol for 24 h. For milling, a plastic jar and zirconia balls were used. After milling the mixtures, the powders were dried. The dried powder mixtures were screened to -325 mesh. The SEM micrographs of milled powders are shown in Fig. 3.

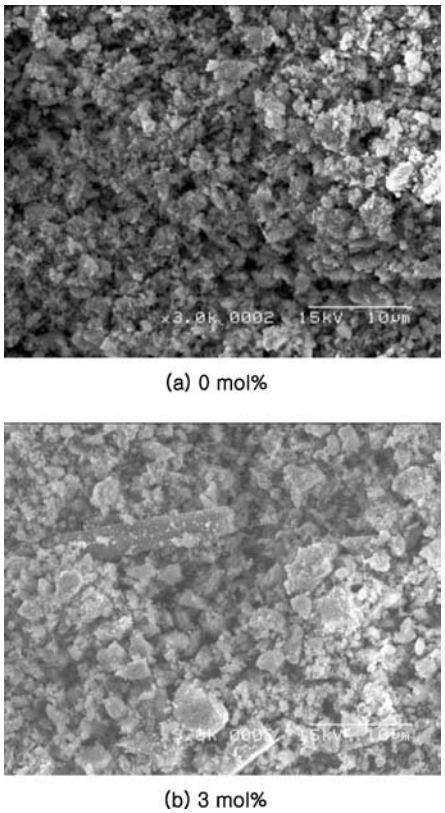

Figure 3 SEM micrographs of milled powders: (a) 0 mol% and (b) 3 mol%.

Fig. 3a shows the SEM micrograph of milled mixtures with no additives. It is shown that the CeO_2 and Gd_2O_3 particles become much finer. The SEM micrograph of milled mixtures with 3 mol% Ga_2O_3 addition is shown in Fig. 3b. The coarse elongated Ga_2O_3 particles were milled remarkably and the mixtures became finer.

The sieved powders of −325 mesh size fraction were uniaxially dry-pressed at 196 MPa into pellets having a diameter of 12 mm and a thickness of 4 mm. After compaction, the compacts were sintered at 1400°C for 5 h. The heating rate was fixed to 10°C/min.

The sintered densities were measured by using the Archimedes method with water and/or calculated from the weights and the dimensions of the specimens. It was found that both methods used for obtaining the density provided almost the same value. An average value obtained from the 5 specimens was taken.

For microstructural investigation, the cross section of the polished specimens was thermally etched. The specimens were then Au-coated and examined with a scanning electron microscope (SEM) (Model S-2400, Hitachi). The elemental distribution was detected utilizing energy dispersive X-ray analysis spectroscopy (EDX) (Model Sigma MS3, Kevex).

X-ray diffraction (XRD) technique was employed to identify the phases and to obtain the values of lattice constant. XRD was performed on the milled powders of specimens by using Rigaku D/MAX IIIA diffractometer with a Ni-filtered Cu K_α radiation.

3. Results and discussion

Fig. 4 shows the sintered density as a function of Ga_2O_3 content. It is shown that the sintered density increased

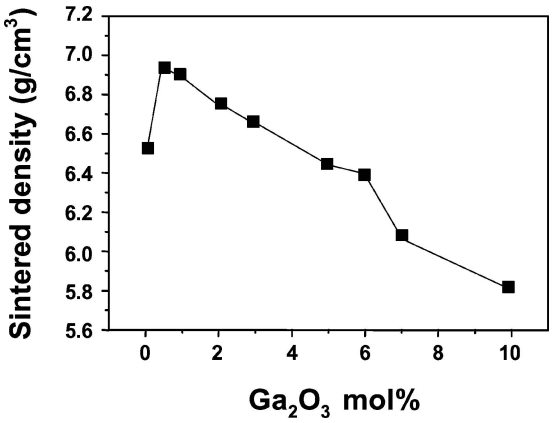

Figure 4 Sintered density as a function of Ga_2O_3 content.

rapidly at 0.5 mol% Ga_2O_3 addition and then it decreases with further addition of Ga_2O_3. The sintered density of the specimen containing 3 mol% Ga_2O_3, however, is higher than that of pure specimen.

The theoretical density of $Ce_{0.8}Gd_{0.2}O_{1.9}$ ceramics was calculated to be 7.263 g/cm^3 by applying the measured lattice parameter of 5.419 Å into the oxygen vacancy model. The sintered density of pure $Ce_{0.8}Gd_{0.2}O_{1.9}$ specimen was 90% of the theoretical density whereas the specimen containing 0.5 mol% Ga_2O_3 had a higher relative density of 96.5%.

These results are compared with those obtained using the coprecipitated powders [15]. For using the coprecipitated powders, the sintered density increased with increasing Ga_2O_3 content up to 5 mol% and then it decreased with further addition of Ga_2O_3 [15].

Fig. 5 shows the SEM micrographs of the polished specimens with different Ga_2O_3 contents. The pure $Ce_{0.8}Gd_{0.2}O_{1.9}$ specimen had an average grain size of 1 μm or less while 0.5 mol% Ga_2O_3-added specimen had a larger average grain size ($\geq 2\mu$m). The grain size of the specimen containing 1 mol% Ga_2O_3 was similar to that of 0.5 mol% Ga_2O_3-added specimen. A decrease in grain size was shown with Ga_2O_3 additions over 1 mol%. The grain size of the specimen containing 3 mol% Ga_2O_3, however, was larger than that of pure specimen. Compared with pure specimen, with Ga_2O_3 additions above 5 mol% the grain size decreased, and porous regions were shown.

For previous study using the coprecipitated powders [15], the grain size increased with increasing Ga_2O_3 content up to 5 mol% and it decreased with further addition of Ga_2O_3. The grain size of the specimen containing 5 mol% Ga_2O_3 was larger than that of 0.5 mol% Ga_2O_3-added specimen in this study.

When the content of Ga_2O_3 is above 2 mol%, grains having a contrast different from ceria grain appear as it is shown on SEM micrographs (Fig. 5d–h). The different grains were identified to be $Gd_3Ga_5O_{12}$ phase by EDX and XRD analyses.

Fig. 6 shows a SEM micrograph and corresponding EDX spectra for the specimen containing 2 mol% Ga_2O_3. The different grain indicated by arrow ⓐ was spot-scanned for EDX analysis, and the result showed high Ga concentration. For arrow ⓑ, high Ce concentration was shown, and it was assigned to be ceria grain.

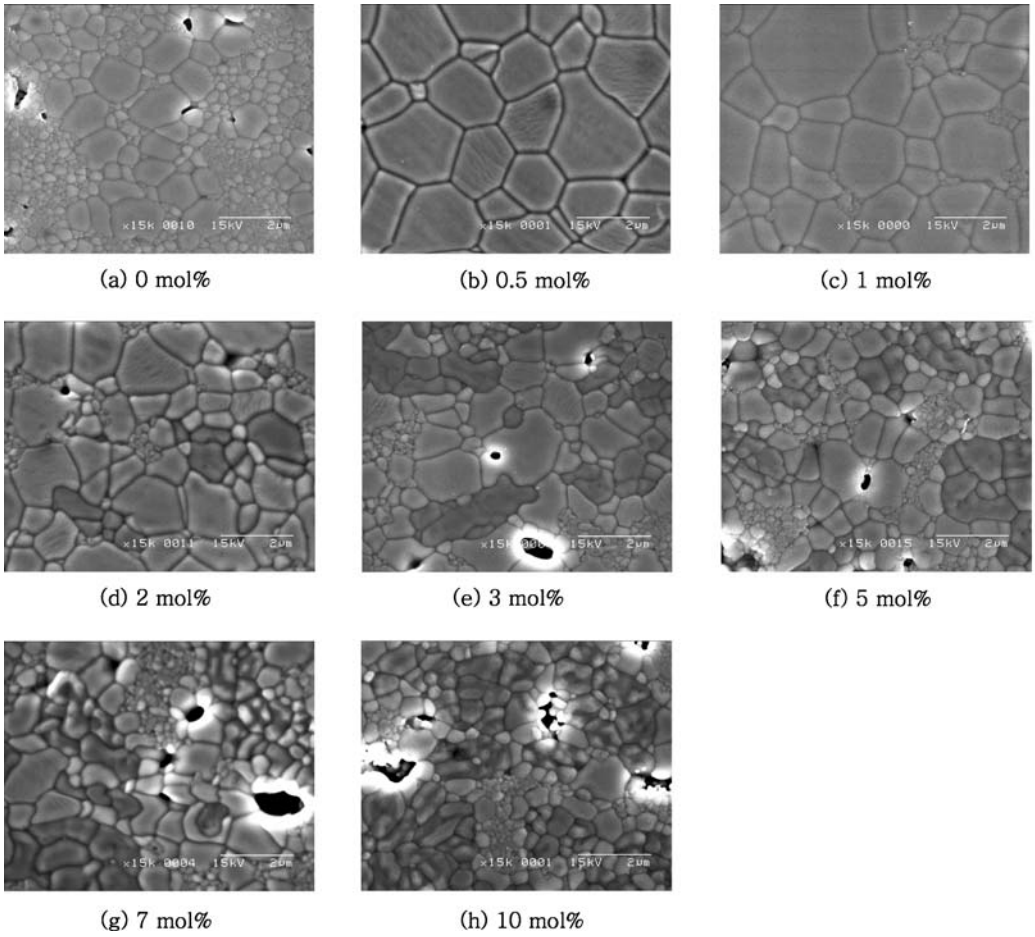

Figure 5 SEM micrographs (×15,000) of the polished specimens with different Ga_2O_3 contents: (a) 0 mol%, (b) 0.5 mol%, (c) 1 mol%, (d) 2 mol%, (e) 3 mol%, (f) 5 mol%, (g) 7 mol%, and (f) 10 mol%.

Fig. 7 shows the XRD patterns of the specimens with different Ga_2O_3 contents. All patterns show the peaks of cubic fluorite type. A series of peaks related with a new phase, however, appear in the addition of Ga_2O_3 content above 3 mol%. These peaks are marked as ♦ in figure. The new phase was identified as $Gd_3Ga_5O_{12}$. With increasing Ga_2O_3 content the peaks of $Gd_3Ga_5O_{12}$ phase became more distinct.

The results of EDX and XRD analyses indicate that the different grains can be assigned to $Gd_3Ga_5O_{12}$ phase. In the case of specimen with 2 mol% of Ga_2O_3 addition, grains having a contrast different from ceria grain appeared on SEM micrograph (Fig. 5d), but the peaks of $Gd_3Ga_5O_{12}$ phase were not detected in XRD pattern probably because of the presence of a small amount.

Yoshida *et al.* [10] reported that gallium samarium garnet ($Ga_5Sm_3O_{12}$) phase was detected as a second phase in the case of samaria-doped ceria with ≥5% gallium addition. They reported XRD peaks of the second phase and a SEM image showing grains having a grain shape different from that of ceria in the case of 5% gallium-added specimen.

Contary to this study, the peaks due to $Gd_3Ga_5O_{12}$ phase were not observed for previous study using the coprecipitated powders [15]. The secondary phases of garnet type were observed only for works using the commercial powders i.e., this study of Gd_2O_3-doped CeO_2 system and Yoshida *et al.*'s study of Sm_2O_3-doped CeO_2 system.

The XRD peaks for Gd_2O_3-doped CeO_2 specimens containing 0.5 mol% Ga_2O_3 were slightly shifted to higher angles compared with those for pure Gd_2O_3-doped CeO_2. The shift to higher angles indicates that the lattice constant is decreased when 0.5 mol% Ga_2O_3 is added. The decrease in lattice constant is considered to be due to the substitution of smaller Ga^{3+} ions (0.61 Å) [16] for Ce^{4+} ions (0.97 Å) [17] in the CeO_2 structure. Thus, we can estimate that Ga_2O_3 is well-dissolved in Gd_2O_3-doped CeO_2 for 0.5 mol% Ga_2O_3 addition.

In general, dopants in alkaline earth oxide-doped ceria systems or rare earth oxide-doped ceria systems have large cation solubilities [17]. However, it is expected that a dissolution of Ga_2O_3 in a CeO_2 system is limited because the ionic radius of Ga^{3+} is much smaller than that of Ce^{4+}. For previous study using the coprecipitated powders, the solubility limit of Ga_2O_3 in $Ce_{0.8}Gd_{0.2}O_{1.9}$ ceramics could be estimated to be nearly 5 mol% at 1400°C [15, 18].

However, it is expected that the equilibrium solubility is limited for this study using the commercial powders where the particle size is large. The limited equilibrium solubility was shown on Sm_2O_3-doped CeO_2 system using the commercial powders [10]. The solubility limit of Ga_2O_3 in Sm_2O_3-doped CeO_2 was 1% at 1450°C [10].

It is noticeable that the distinct differences between this study using the commercial powders and another using the coprecipitated powders are shown in the variation in sintered density, the appearance of a secondary

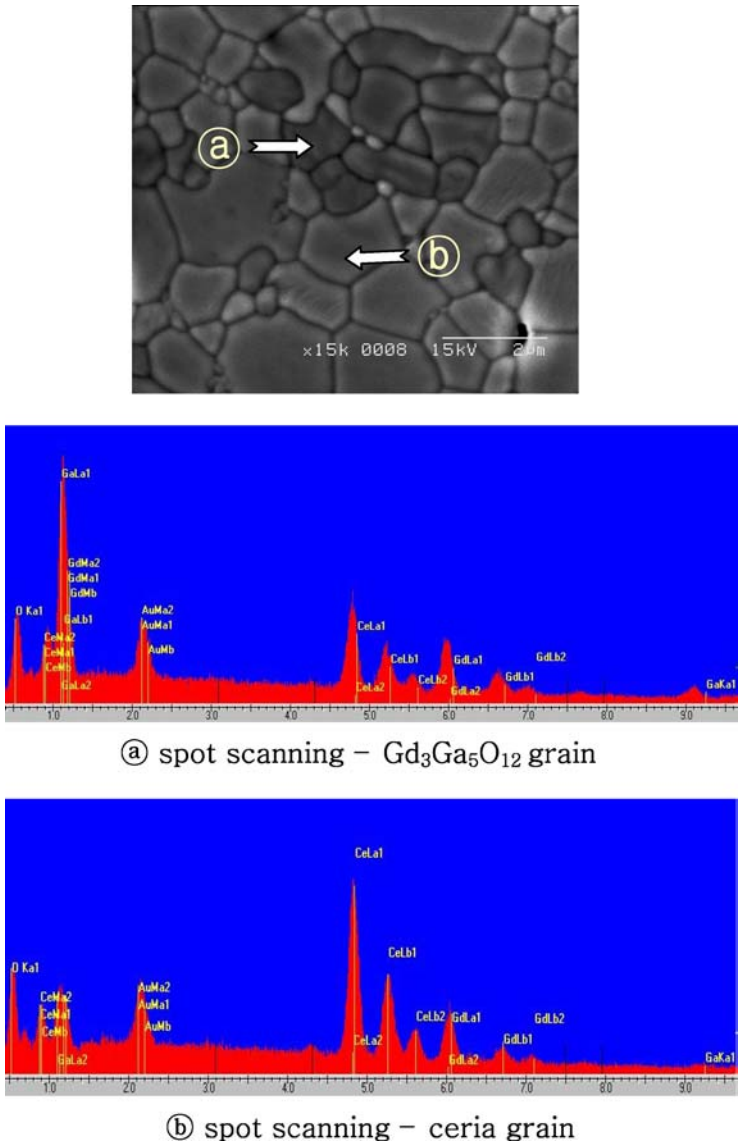

Figure 6 SEM micrograph (×15,000) and corresponding EDX spectra for Gd_2O_3-doped CeO_2 containing 2 mol% Ga_2O_3.

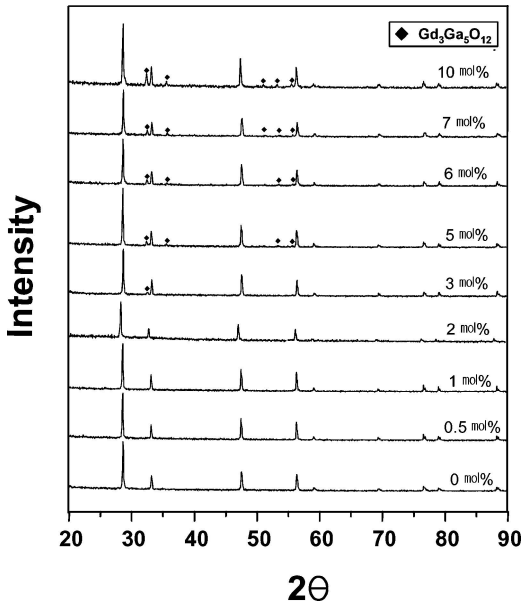

Figure 7 X-ray diffraction patterns of the sintered specimens with different Ga_2O_3 contents.

phase, and the solid solubility limit. In the case of using the coprecipitated powders the sintered density increased with increasing Ga_2O_3 content up to 5 mol% and then it decreased with further addition of Ga_2O_3. Moreover, the equilibrium solubility was 5 mol% and the secondary phase did not appear.

However, for this study employing the commercial powders, the sintered density increased rapidly at 0.5 mol% Ga_2O_3 addition and the limited equilibrium solubility was shown. Furthermore, a secondary phase of $Gd_3Ga_5O_{12}$ appeared. When employing the coprecipitated powders, the increase in the solubility limit and the lack of a secondary phase are probably due to the use of fine powders prepared by the coprecipitation method, which were mixed homogeneously at the atomic level.

As noted previously, it is possible that Ga_2O_3 additions resulted in the substitution of Ga^{3+} ions for Ce^{4+} ions within its solubility limit. The addition of Ga_2O_3 in a CeO_2 system would lead to the formation of oxygen vacancies because of charge compensation. It is expected that these oxygen vacancies enhance the

densification rate and promote the grain boundary mobility. Moreover, the addition of Ga_2O_3 may induce the large distortion of the surrounding lattice because Ga^{3+} ion has much smaller size compared with that of Ce^{4+} ion. It is also expected that the lattice distortion promotes the grain boundary mobility due to the effect of severely undersized dopant [17].

The sintered density was the highest at 0.5 mol% Ga_2O_3 addition and the grain size was the largest at that addition. These results indicate that Ga_2O_3 additions within the solubility limit accelerate the densification rate remarkably and promote the grain boundary mobility.

However, at a higher Ga_2O_3 content above 2 mol%, $Gd_3Ga_5O_{12}$ is precipitated. The precipitates inhibit the grain growth and lead to the decrease in grain size by a pinning effect. The precipitates cause the decline in density probably because the strain is produced due to the difference in both the elastic modulus and the thermal expansion coefficient between the precipitates and CeO_2.

The addition of Ga_2O_3 up to the solid solubility limit promoted the grain growth and densification. It is suggested that soluble Ga_2O_3 has an affirmative effect on the sintering behavior of $Ce_{0.8}Gd_{0.2}O_{1.9}$ ceramics prepared by commercial powders.

4. Conclusion

The effects of gallia additions on the sintering behavior of $Ce_{0.8}Gd_{0.2}O_{1.9}$ ceramics were investigated by the use of commercial powders. Sintered density increased rapidly at 0.5 mol% Ga_2O_3 addition. However, it decreased with further addition of Ga_2O_3. Grain size also increased at 0.5 mol% Ga_2O_3 addition but it decreased with further addition of Ga_2O_3 in a way similar to the density. The sintered density of the specimen containing 3 mol% Ga_2O_3, however, was higher than that of pure specimen. At a higher Ga_2O_3 content above 2 mol%, grain size decreased by a pinning effect induced by $Gd_3Ga_5O_{12}$ precipitates. The addition of Ga_2O_3 caused the promotion of grain growth and an increase in density. It is suggested that Ga_2O_3 addition gives an affirmative effect on the sintering behavior of $Ce_{0.8}Gd_{0.2}O_{1.9}$ ceramics prepared by commercial powders.

Acknowledgements

This work was supported by ECC (Electronic Ceramics Center) at Dong-eui University as RRC • TIC program.

References

1. B. RILEY, *J. Power Sources* **29** (1990) 223.
2. J. V. HERLE, T. HORITA, T. KAWADA, N. SAKAI, H. YOKOKAWA and M. DOKIYA, *J. Amer. Ceram. Soc.* **80** (1997) 933.
3. A. OVERS and I. RIESS, *ibid.* **65** (1982) 606.
4. P. L. CHEN and I. W. CHEN, *ibid.* **76** (1993) 1577.
5. Y. C. ZHOU and M. N. RAHAMAN, *J. Mater. Res.* **8** (1993) 1689.
6. K. YAMASHITA, K. V. RAMANUJACHARY and M. GREENBLATT, *Solid State Ionics* **81** (1995) 53.
7. A. K. BHATTACHARYA, A. HARTRIDGE, K. K. MALLICK and J. L. WOODHARD, *J. Mater. Sci.* **31** (1996) 5005.
8. J. V. HERLE, T. HORITA, T. KAWADA, N. SAKAI, H. YOKOKAWA and M. DOKIYA, *Solid State Ionics* **86–88** (1996) 1255.
9. K. HIGASHI, K. SONODA, H. ONO, S. SAMESHIMA and Y. HIRATA, *J. Mater. Res.* **14** (1996) 957.
10. H. YOSHIDA, K. MIURA, J. FUJITA and T. INAGAKI, *J. Amer. Ceram. Soc.* **82** (1999) 219.
11. C. M. KLEINLOGEL and L. J. GAUCKLER, *Solid State Ionics* **135** (2000) 567.
12. *Idem.*, *J. Electroceram.* **5** (2000) 231.
13. T. ZHANG, P. HING, H. HUANG and J. KILNER, *J. Europ. Ceram. Soc.* **21** (2001) 2221.
14. *Idem.*, *ibid.* **22** (2002) 27.
15. J. S. LEE, K. H. CHOI, B. K. RYU, B. C. SHIN and I. S. KIM, *Mater. Res. Bull.* **39** (2004) 2025.
16. R. D. SHANNON and C. T. PREWITT, *Acta Cryst. B* **25** (1969) 925.
17. P. L. CHEN and I. W. CHEN, *J. Amer. Ceram. Soc.* **79** (1996) 1793.
18. J. S. LEE, K. H. CHOI, B. K. RYU, B. C. SHIN and I. S. KIM, *J. Mater. Sci. Lett.* **22** (2003) 1805.

Received 29 August
and accepted 26 October 2004